

Synthesis of Super Hydrophobic Clay by Solution Intercalation Method from Aqueous Dispersions

M. ACIKYILDIZ^a, A. GURSES^{b,*}, H.H. YOLCU^c

^aKilis 7 Aralık University, Faculty of Science and Art, Dep. of Chemistry, 79000, Kilis, Turkey

^bAtatürk University, K.K. Education Faculty, Dep. of Chemistry, 25240, Erzurum, Turkey

^cKafkas University, Education Faculty, Dep. of Chemistry, 36100, Kars, Turkey

The super hydrophobic materials have inspired a great deal of interest and research in recent years because of their unique water-repellent, self-cleaning properties, and their potential for practical applications. This study aims to create a super hydrophobic clay surface from aqueous dispersions of a long-chain hydrocarbon, *Cetyltrimethylammonium Bromide* (CTAB), and layered silicate via the solution intercalation method. First, to increase diffusing tendency of CTA⁺ ions from aqueous medium to the interlayer region of clay, long-chain hydrocarbon agent was dispersed in aqueous surfactant solution via hydrophobic interactions between the tails of CTA⁺ ions and hydrocarbon chains. Then, the adsorption of the long tailed ions of CTAB on the surface of the clay layers was carried out. Effects of variables, such as temperature, initial surfactant concentration and hydrocarbon dosage onto the adsorbed amount of CTA⁺ ions were investigated by considering the zeta potentials and contact angle values of organo-clay particles. The results show that by intercalation of the long tailed CTA⁺ ions to the interlayer galleries of clay, high hydrophilic clay can be possible to convert to super hydrophobic clay. Also, the static contact angle values of organo-clay particles progressively increase with the increasing amount of hydrocarbon. The static contact angle value of powder organo-clay is about 150°, indicating its super hydrophobic character. XRD pattern and HRTEM images for the organo-clay confirm the intercalated structures.

DOI: [10.12693/APhysPolA.127.1156](https://doi.org/10.12693/APhysPolA.127.1156)

PACS: 81.07.Pr, 61.43.Gt, 68.08.Bc, 68.35.Ct

1. Introduction

Many surfaces in nature are highly hydrophobic and self-cleaning (*e.g.* water striders, butterflies and cicada). Non-wettable surfaces with high water contact angle and facile sliding of drops are called super hydrophobic surfaces. Solid substrates, of which surface wetting ability can be reversibly switched, have attracted much attention recently, because of their importance in the fabrication of smart devices [1, 2]. Self-cleaning surfaces find many applications in satellite dishes, solar energy panels, paints, exterior architectural glass and green houses, and heat transfer surfaces in air conditioning equipment [3]. Surfaces with a high degree of roughness and with low surface energy show super hydrophobicity [4, 5]. Techniques to produce super hydrophobic surfaces can be simply divided into two categories: by making a rough surface from a low-surface-energy material and modifying a rough surface with a material of low surface energy, respectively [3]. The synthesis and applications of new kinds of super hydrophobic and self-cleaning organic or inorganic material are essential and important tasks to fulfill [1]. Clay minerals are low-cost materials and also play a very important role as constituents of soil. Due to their great cation exchange capacity and their structure-building properties, they deeply influence the physico-chemical and environmental properties of soil [6]. In re-

cent years, clays are important in many different fields such as agriculture, oil drilling, engineering applications including road construction, dam construction, and waste containment [7, 8].

Clays are widely used as adsorbents due to their high specific surface area. In their natural forms, clays have only a weak sorption capacity of hydrophobic organic compounds from aqueous solutions because of the strong hydration of their inorganic exchangeable ions. Exchange of the inorganic ions with organic cations renders clay surfaces hydrophobic and greatly enhances clays' adsorptive capacities towards the hydrophobic organic compound [9, 10]. It is also a cheap sorbent, one of the most economic and efficient means of cleaning up hydrocarbon spills on the shoreline or land [11]. Many studies investigate organo-clay sorptive characteristics towards the hydrophobic organic compound [11–15]. Expansion of phyllosilicates with organo-cations, such as alkyl ammonium cations and delamination or exfoliation of layered solids has been widely studied [16, 17]. The intercalation of long-chain organic cations into interlayer regions of the clay, changes the surface of the clay particles from hydrophilic or organophilic to hydrophobic or organophobic [18]. Expansion degree of basal spacing between the clay platelets depends on the chain length of the organic molecules and on their conformation in the interlayer region [17, 19].

This study aims to form super hydrophobic clay surface using aqueous dispersions of a long-chain hydrocarbon, *Cetyltrimethylammonium Bromide* (CTAB), and layered silicate via the solution intercalation method. The ef-

*corresponding author; e-mail: ahmetgu@yahoo.com

fects of factors, such as the initial CTAB concentration, hydrocarbon dosage, and temperature on the variation of hydrophobicity of the clay surfaces were investigated by using measurements of static contact angle. In addition, the prepared organo-clay samples were characterized by XRD analysis, zeta potential measurements, and static contact angle measurements.

2. Experimental

2.1. Material

In this study, cationic surfactant, Cetyltrimethylammonium Bromide (CTAB) (hexadecyltrimethylammonium bromide) was used to synthesize organophilic clay and to disperse long-chain hydrocarbon agent in water. The clay sample taken from Erzurum region in Turkey, includes both clay and non-clay minerals. The sample consists of smectite (26%), chlorite (20%), illite (17%), and kaolinite (14%) (clay minerals) as well as analcime (11%), calcite (7%), quartz (3%) and feldspar (3%) (non-clay minerals). The cation exchange capacity (CEC) of the clay was determined by the methylene blue test (ANSI/ASTM C837-76). Tables I and II show several properties of clay and long-chain hydrocarbon, respectively. All chemicals used in this study were supplied from Merck.

Some physical properties of clay sample.

TABLE I

CEC* [meq/100g]	d^* [g/cm ³]	OMC* [%]	Liquid limit w_L , [%]	Plastic limit w_P , [%]	Plasticity index I_p	a^* [m ² /g]
48.9	2.61	5.10	102.00	35.00	67.00	64.20

*(CEC) Cation exchange capacity, (d) specific gravity, (OMC) organic matter content, (a) specific surface area

Some physical and chemical properties of long-chain hydrocarbon used in this study.

TABLE II

Density (15 °C) [kg/m ³]	Calorific value [MJ/kg]	Flash point [°C]	Water by distillation [wt.%]	C	H	N	S	Ash
990.7	42.74	105.8	0.1	83.4	11.9	0.8	1.5	0.03

XRD measurements of the raw and organo-clay samples were performed using Rigaku SmartLab X-ray Diffractometer with a CuK α (1.540 Å) radiation, operating at 40 kV and 30 mA over a 2θ range of 3–40°. In order to estimate the textural rearrangement of raw and modified clays, the specimens from the samples were examined by using a JEOL JEM 2100F High Resolution Transmission Electron Microscope operated at 200 kV. Chemical composition of the clay sample was determined by Rigaku RIX-3000 X-Ray Fluorescence spectrometry (Rigaku Corporation, Tokyo, Japan) (see Table III).

Chemical composition of clay sample.

TABLE III

SiO ₂	Al ₂ O ₃	CaO	MgO	Fe ₂ O ₃	K ₂ O	Na ₂ O	TiO ₂	SO ₃	P ₂ O ₅
45.12	13.70	7.48	7.29	5.63	2.62	2.37	0.53	0.44	0.25

2.2. Preparation of modified clay

The combination of swelling and adsorption processes during intercalation and exfoliation of layered silicates was used for solution intercalation. The clay sample was purified by washing, dried in vacuum oven and sieved to give a 38–85 μ m size fraction using ASTM sieves. 0.3 g of long-chain hydrocarbon agent was dispersed in 500 ml of CTAB aqueous solution (240 mg/l) for 30 minutes. After addition of 1.0 g raw clay to the prepared dispersion, it was shaken at shaking speed of 200 rpm and at various temperatures (293, 313, and 333 K), using a thermostatic shaker for 30 minutes. Finally, the mixture was filtered and then dried in a vacuum oven at 383 K for 2 hours. The concentrations of CTA⁺ in the supernatant, after the adsorption, were determined using a double-beam UV spectrophotometer at 375 nm in a company with 0.02 ml of 0.1% picric acid in 0.002 M NaOH and 0.40 ml of 1,2-dichloroethane added per 1.0 ml of the supernatant [20]. The calibration curve was found to be very reproducible and linear over the concentration range used in this study. The amount of adsorbed CTAB was calculated from the concentrations in solution before and after the adsorption. Blanks containing no CTAB were used for each series of experiments.

2.3. Zeta potential measurements

The zeta potential measurements of solid particles in suspensions were carried out using a Zeta Meter 3.0+ (Zeta-Meter, Inc., Staunton, VA, USA) at unadjusted pHs. The zeta potential values were corrected for temperature differences using the following equation,

$$\zeta_d(\text{mV}) = C_T \zeta_0, \quad (1)$$

where ζ_d , C_T , ζ_0 represent the corrected zeta potential value, correction factor related to temperature and the measured zeta potential value, respectively.

2.4. Static contact angle measurements

The static contact angle measurements of organo-clay samples were conducted in two different ways. First, a pellet was prepared under 1.06 ton/cm² pressure, using 0.6 g of organo-clay sample. Second, powder organo-clay sample was deposited over a glass plate. A static contact angle measurement was performed using a CAM-101 optical contact angle analyzer (KSV Instruments, Finland). The static contact angles were measured by using goniometer, which uses a water drop of 6 μ l. Young-Laplace equation has been taken into account at solid-liquid interface. Each of the pictures which were taken at a constant rate (1 frame/second) was repeated four times, for the total amount of five frames.

3. Results and discussions

3.1. Characterization of modified organo-clay

Figure 1 shows the XRD patterns for samples: the raw clay (RC) and the organo-clays which were modified with CTAB concentration of 240 mg/l (OC), and by addition to the same CTAB concentration of a constant amount of long-chain hydrocarbon (0.3 g/1.0 g clay) (HOC).

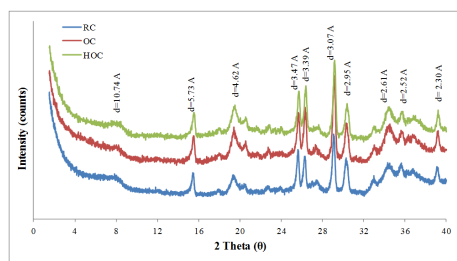


Fig. 1. The XRD patterns for the RC, OC, and HOC samples (labeled with RC's d space values).

The raw clay is a mixture of different clay minerals, which contains smectite and illite as layered silicates. The characteristic peak of smectite in Fig. 1 exhibits a marked shift to the left, if compared with the raw clay, in the case of the clay modified by addition to the initial CTAB concentration of 240 mg/l, of a constant amount of long-chain hydrocarbon (0.3 g/1.0 g clay), while it shows no significant change in the case of the clay modified with the initial CTAB concentration of 240 mg/l, without the addition of hydrocarbons. The shift can be attributed to the intercalation of the long tailed CTA^+ ions which were attached long-chain hydrocarbon molecules into interlayer region of layered silicates, indicating partly an increase in the basal spacing ($\Delta d \approx 0.2$ nm). This difference in the basal spacing between the cases with and without the addition of hydrocarbons in comparison with the raw clay implies that the addition of hydrocarbon does not lead to any changes in terms of the mechanism of the adsorption.

Moreover, the organo-clay modified by the addition of a constant amount of long chain hydrocarbon (0.3 g/1.0 g clay) into the CTAB solution (240 mg/l), has exhibited a dramatically lower specific surface area ($1.34 \text{ m}^2/\text{g}$), compared to that of the raw clay (see Table I). The HRTEM images also confirm that there is a significant change in the surface area of organo-clay and hence in its morphology. HRTEM images of the same samples are given in Fig. 2.

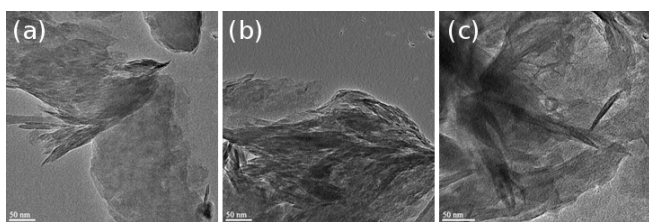


Fig. 2. The HRTEM images for RC (a), OC (b), and HOC (c) samples.

From Fig. 2, it can be seen that the clay platelets in both modified specimens (Fig. 2b and 2c) emerged as the sequenced ensembles separated from each other. One can compare these with the plates of the raw clay in Fig. 2a. The last HRTEM image (Fig. 2c) also, shows the presence of some individual tactoids and the stacks of clay platelets. These results are consistent with literature results [21–25].

3.2. Effect of initial CTAB concentration

In order to investigate the effect of the initial CTAB concentration on the hydrophobicity of the clay, 0.3 g of long-chain hydrocarbon agent was dispersed in the aqueous solution of CTAB (100, 200, 240, 260, 300, and 320 mg/l) of 500 ml, and shaken in a thermostatic shaker at 293 K for 30 minutes. After addition of 1.0 g of raw clay to the prepared dispersion, it was shaken at 200 rpm shaking speed and 293 K, using a thermostatic shaker for 30 minutes. Finally, the mixture was filtered and, then dried in a vacuum oven at 383 K for 2 hours. The variation of the adsorbed amount of CTAB, the zeta potential of particles, and the static contact angle of organo-clay, which may determine the hydrophobicity of clay, with equilibrium CTAB concentrations is shown in Fig. 3.

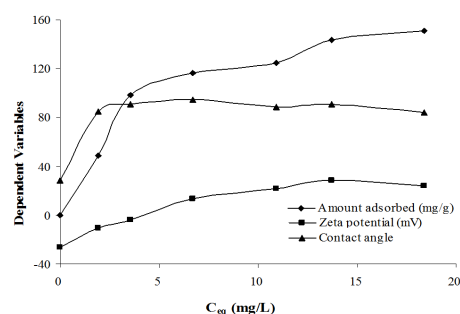


Fig. 3. The change of the variables such as, the adsorbed amount of CTAB, the zeta potential of particles, and the static contact angle of organo-clay with the equilibrium CTAB concentration.

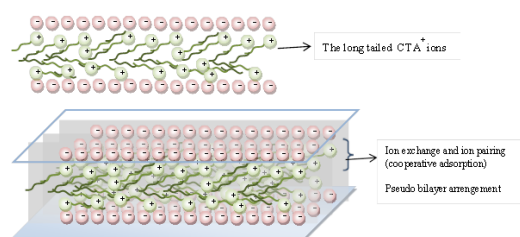


Fig. 4. The probable orientations of the long tailed CTA^+ ions to which were attached long-chain hydrocarbon molecules in the interlayer region of layered silicates.

The probable orientations of the CTA^+ ions, which have bonded with long-chain hydrocarbon molecules, in the interlayer region of the layered silicate, are schematically shown in Fig. 4. As the equilibrium CTAB concentration has been increased (see Fig. 3), the adsorption efficiency has first increased and then has formed two progressive plateaus. The observed higher adsorption efficiency at the lower CTAB equilibrium concentrations can be attributed to effective interactions between charged sites in the surface of clay platelet and the long tailed CTA^+ ions, due to the existence of more unoccupied active sites and their easier transfer onto the interlayer region [26, 27]. Therefore, it can be argued that the adsorption of the long tailed CTA^+ ions onto the active sites is more favorable than existence of

free CTA^+ ions, because their tendency of escaping from the bulk to the interlayer region has increased. The increase of equilibrium CTAB concentration leads to the surface saturation through the ion exchange and the ion-pairing mechanisms [28]. In the first plateau, the values of the zeta potential of clay platelets are close to the value of about 0 mV (240 mg/l initial concentration of CTAB), which caused the higher interface tension of organo-clay/aqueous suspension. A further increase in the equilibrium CTAB concentration may cause the formation of second plateau by cooperative adsorption or hemi-micelle formation, via the interactions between the tails of adsorbed ions and the hydrophobic tails of the free ions [20, 28–30]. The formation of second plateau, which has emerged in the range of the higher equilibrium CTAB concentrations (> 240 mg/l initial CTAB concentration) of CTAB, can be considered as a result of hydrophobic binding, after the surface saturation and the formation of hemi-micelle. Probably the predominant adsorption mechanism is the hydrophobic binding [30, 31], in which the driving force is the increase in the entropy of the system. However, Fig. 3 shows that the static contact angle values measured for the organo-clay are almost independent from the equilibrium CTAB concentration, after reaching to the zero point of charge (zpc) of the particles.

3.3. The effect of hydrocarbon dosage

In order to investigate the effect of hydrocarbon dosage on some properties of organo-clay, a 500 ml aqueous solution of CTAB (240 mg/l) was mixed with several amounts of hydrocarbon (0.05, 0.1, 0.2, 0.3, 0.4, 0.5, 0.65, 0.7, 0.75, 0.9, and 1.0 g) and shaken at 293 K for 30 minutes in a thermostatic shaker. Then 1.0 g of clay sample was added to this dispersion and it was shaken for 30 minutes at 200 rpm. The mix was filtered, and the modified clay samples were dried in a vacuum oven at 383 K for 2 h.

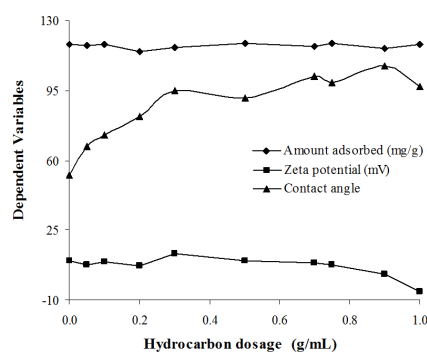


Fig. 5. Variation of the amount of adsorbed CTAB, the zeta potential and the contact angle values, with the dosage of hydrocarbon.

Figure 5 shows the variation of the amount of adsorbed CTAB, the zeta potential and the contact angle values, with the increasing dosage of the hydrocarbon. This figure shows that the efficiency and effectiveness of adsorption of CTAB do not change significantly with the increase of amount of long-chain hydrocarbon. Therefore,

it could be said, that the electrostatic interactions between the active sites on the surface of clay platelet and the long tailed CTA^+ ions is predominant and is responsible for charge neutralization.

3.4. The effect of temperature

In order to investigate the effect of temperature on the amount of adsorbed CTAB, on the zeta potential and on the contact angle values of organo-clay, the adsorption experiments were carried out after the dispersion of hydrocarbon (0.3 g/1.0 g clay) in a 500 ml aqueous solution of CTAB (240 mg/l) for 30 minutes at 293, 313 and 333 K (see Fig. 6).

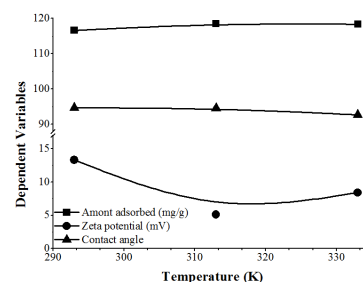


Fig. 6. The variation of the amount of adsorbed CTAB, the zeta potential and the contact angle values with temperature.

Figure 6 reveals that as the temperature increased, the amount of adsorbed long-tailed CTA^+ ions increased and a more stable dispersion of the hydrocarbon agent in water occurred, indicating that these processes are endothermic, in nature.

This figure also shows that the static contact angle values have partly decreased with the increasing temperature, while their zeta potential values have initially decreased and then slightly increased. This can be explained by considering two competing factors, i) the viscosity of long-chain hydrocarbon, which is a viscous liquid, decreases as the temperature increases, and thus the interactions between CTA^+ ions and hydrocarbon molecules may occur more effectively and a lot of CTA^+ ions may be trapped in the agglomerates of the hydrocarbon molecules, ii) the increase of temperature may improve the transport of free CTA^+ ions from the bulk phase into the interlayer region of the clay and so lead to an increase in the zeta potential values of the particles.

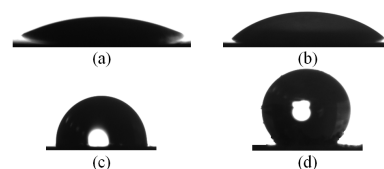


Fig. 7. Pictures of water droplets on RC (a), OC (b), HOC (c), and powdered HOC (d) samples.

Figure 7 shows pictures of water droplets on the raw clay, on the compacted samples of organo-clays, which were modified using dispersion without/with long-chain hydrocarbon agent at CTAB concentration of 240 mg/l,

and on the powdered sample modified with long-chain hydrocarbon agent at CTAB concentration of 240 mg/l. These revealed that the droplet shape on the powdered sample is almost spherical and it has a static contact angle of more than 150° , whereas the static contact angles measured on other samples are about 100° or less. The higher static contact angle value, measured on the powdered sample can be attributed to the lotus effect, which can be based on the looseness of the tails of the long tailed adsorbed ions [32, 33].

4. Conclusions

This study aims to create a super hydrophobic clay surface from aqueous dispersions of a long-chain hydrocarbon, Cetyltrimethylammonium Bromide (CTAB), and layered silicate, via the solution intercalation method. The main findings of the study could be summarized as follows:

- The XRD patterns and HRTEM images of the samples indicate that the intercalation of the long tailed CTA⁺ ions, which were attached long-chain hydrocarbon molecules, into interlayer region of layered silicates has occurred and thus has partly increased the basal spacing ($\Delta d \approx 0.2$ nm).
- The adsorption of the long tailed CTA⁺ ions onto the active sites is more favorable than existence of free CTA⁺ ions, because their escaping tendency from the bulk to the interlayer region has increased.
- The static contact angle values measured for the organo-clay are almost independent from the equilibrium CTAB concentration after reaching the zero point of charge (zpc) of the particles.
- The efficiency and effectiveness of adsorption of CTAB do not change significantly with the increase of amount of long-chain hydrocarbon. Therefore, it could be said that the electrostatic interactions between the active sites on the surface of clay platelet and the long tailed CTA⁺ ions is predominant and is responsible for charge neutralization.
- The droplet shape on the powdered sample is almost spherical and it has a static contact angle of more than 150° , whereas the static contact angle measured on other the samples is about 100° or less. The higher static contact angle value measured on the powdered sample can be attributed to the lotus effect.

References

- [1] X. Feng, L. Jiang, *Adv. Mater.* **18**, 3063 (2006).
- [2] Y. Ofir, B. Samanta, P. Arumugam, V.M. Rotello, *Adv. Mater.* **19**, 4075 (2007).
- [3] M. Ma, R.M. Hill, *Curr. Opin. Colloid. In. Sci.* **11**, 193 (2006).
- [4] R. Mohammadi, J. Wassink, A. Amirfazli, *Langmuir* **20**, 9657 (2004).
- [5] Z.G. Guo, J. Fang, J.C. Hao, Y.M. Liang, W.M. Liu, *Chem. Phys. Chem* **7**, 1674 (2006).
- [6] M.O. Adebajo, R.L. Frost, J.T. Kloprogge, O. Carmody, S. Kokot, *J. Porous Mat.* **10**, 159 (2003).
- [7] I. McKissock, E.L. Walker, R.J. Gilkes, D.J. Carter, *J. Hydrol.* **231-232**, 323 (2000).
- [8] C. Bilgiç, *J. Colloid Interf. Sci.* **281**, 33 (2005).
- [9] W.P. Gates, A. Nefiodovas, P. Peter, *Clay Clay Miner.* **52**, 192 (2004).
- [10] L. Xu, L. Zhu, *J. Colloid Interf. Sci.* **331**, 8 (2009).
- [11] O. Carmody, R. Frost, Y. Xi, S. Kokot, *J. Colloid Interf. Sci.* **305**, 17 (2007).
- [12] O. Carmody, R. Frost, Y. Xi, S. Kokot, *Surf. Sci.* **601**, 2066 (2007).
- [13] T.S. Anirudhan, M. Ramachandran, *Appl. Clay Sci.* **35**, 276 (2007).
- [14] R. Zhu, L. Zhu, J. Zhu, L. Xu, *Sep. Purif. Technol.* **63**, 156 (2008).
- [15] L. Zampori, P. Gallo Stampino, G. Dotelli, *Appl. Clay. Sci.* **42**, 605 (2009).
- [16] Q. Huang, W. Wang, Y. Yue, W. Hua, Z. Gao, *J. Colloid Interf. Sci.* **257**, 268 (2003).
- [17] A. Pérez-Santano, R. Trujillano, C. Belver, A. Gil, M.A. Vicente, *J. Colloid Interf. Sci.* **284**, 239 (2005).
- [18] R. Guegan, M. Gautier, J.M. Beny, F. Muller, *Clay Clay Miner.* **57**, 502 (2009).
- [19] J. Hrachová, P. Komadel, I. Chodák, *Clay Clay Miner.* **57**, 444451 (2009).
- [20] M.J. Rosen, H.A. Goldsmith, *Systematic Analysis of Surface-Active Agents*, Wiley-Interscience, New York, 1972.
- [21] H. Khalaf, O. Bouras, V. Perrichon, *Microporous Mater.* **8**, 141 (1997).
- [22] Q. Zhou, R.L. Frost, H. He, Y. Xi, *J. Colloid Interf. Sci.* **314**, 405 (2007).
- [23] L. Wang, A. Wang, *J. Hazard. Mater.* **160**, 173 (2008).
- [24] B. Schampera, S. Dultz, *Clay Clay Miner.* **59**, 42 (2011).
- [25] A.K. Mishra, S. Allauddin, R. Narayan, T.M. Aminabhavi, K.V.S.N. Raju, *Ceram. Int.* **38**, 929 (2012).
- [26] A. Gürses, M. Yalçın, M. Sözbilir, C. Doğar, *Fuel Process. Technol.* **81**, 57 (2003).
- [27] M. Alkan, M. Karadas, M. Dogan, Ö. Demirbas, *J. Colloid Interf. Sci.* **291**, 309 (2005).
- [28] M.J. Rosen, *J. Am. Oil Chem. Soc.* **52**, 431 (1975).
- [29] A. Gürses, S. Karaca, M. Açıkıldız, M. Ejder, *Chem. Eng. J.* **147**, 194 (2009).
- [30] A. Gürses, K. Güneş, F. Mindivan, M. Ejder Korucu, M. Açıkıldız, Ç. Doğar, *App. Surf. Sci.* **318**, 79 (2014).
- [31] Q. Liu, S. Zhang, D. Sun, J. Xu, *Colloid Surface A.* **338**, 40 (2009).
- [32] D.M. Spori, T. Drobek, S. Zürcher, M. Ochsner, C. Sprecher, A. Mühlebach, N.D. Spencer, *Langmuir* **24**, 5411 (2008).
- [33] A. Marmur, *Langmuir* **19**, 8343 (2003).